*International Journal of Engineering & Technology*, 9 (3) (2020) 621-629

International Journal of Engineering & Technology

*Website: www.sciencepubco.com/index.php/IJET*

***Research paper***

# Effect of design parameters of dental implant on stress distribution: a finite element analysis

**Pooyan Rahmanivahid [1] *, Milad Heidari [1]**

[1] *Mechanical Engineering and Vehicle Technology Department, Global College of Engineering and Technology (GCET), P.O. Box 2546 CPO Ruwi 112, Muscat, Sultanate of Oman*

**Corresponding author E-mail: pooyan@gcet.edu.om*

**Abstract**

Nowadays, root osseointegrated dental implants are used widely in dentistry mainly for replacement of the single missing tooth. The success rate of osseointegrated dental implants depends on different factors such as bone conditions; surgery insertion technique, loading history, and biomechanical interaction between jawbone and implant surface. In recent years, many studies have investigated design factors using finite element analysis with a concentration on major parameters such as diameter, pitch, and implant outlines in the distribution of stress in the bone-implant interface. There is still a need to understand the relationship and interaction of design factors individually with stress distribution to optimize implant structure. Therefore, the present study introduced a new dental implant and investigated the effect of design parameters on stress distribution. The finite element modeling was developed to facilitate the study with a comparison of design parameters. Boundary and loading conditions were implemented to simulate the natural situation of occlusal forces. Based on results, V-shape threads with maximum apex angle caused a high rate of micro-motion and high possibility of bone fracture. Low Von-Mises stress was associated with low bone growth stimulation. Besides, small fin threads did not integrate with cancellous bone and consequently lower stress accommodation. V-5 fin had no extraordinary performance in cancellous bone. Small surface areas of fins did not integrate with the surrounding bone and high-stress concentration occurred at the tail. These fins are recommended as threads replacement. It was concluded that the implant structure had less influence on stress distribution under horizontal loading.

***Keywords***: *Finite Element Analysis; Stress Distribution; Micro-Motion; Dental Implant.*

## 1. Introduction

Osseointegration is defined as the direct anchorage of a biocompatible fixture in the human bone. Nowadays, root osseointegrated dental implants are used widely in dentistry mainly for replacement of the single missing tooth. Osseointegrated dental implants have shown a high success rate in clinical investigations. However, the success rate depends on different factors such as bone conditions; surgery insertion technique, loading history, and biomechanical interaction between jawbone and implant surface.

Dental implant systems are used for the replacement of partially or fully edentulous patients. For a single tooth replacement in molar or premolar region where implants stand in a straight line under large masticatory forces, high strength values for implant material is advised. Implants with lower strength values could be used for full arch replacement where implants are located in a horseshoe formation that provides maximum strength and stability [1, 2].

Current dental implants in the market have been made of metal alloys covered by biocompatible surface coating to improve the healing process and osseointegration. Since the integration of bone-implant has been highlighted in dentistry investigations, improving implant design depends on the ability to predict mechanical reactions and remodeling response of bony tissues around implants [3].

With the development of computational technologies, nowadays researchers can predict a long term oral bone remodeling around implants by use of the Finite element analysis (FEA) method. Even though some studies have compared FEA results with clinical documents such as X-ray images or computerized tomography '(CT) scans, still there is a lack of feasibility and accuracy of remodeling algorithms [4].

Dental implants are inserted directly into Jawbone and continuous bone remodeling maintains interface stability in the contact area. Bone-implant interface mechanical status is the most significant factor in the stability of implants. There is a certain induced strain threshold of 50 to 150 μm that regulates interface response [5]. Root form osseointegrated dental implants consist of a ceramic crown similar to missing tooth shape, an abutment to connect the crown to implant root, and a root-form implant made of a biocompatible material to osseointegrate with bony tissues. Implant failure is associated with bone fracture as a consequence of high-stress concentration mainly around first threads. The failures areas of the interface are due to exceeding either the material yield strength or unbearable level of stress and strain.

The majority of implants in the market have a cylindrical or conical screw shape root, provided in different sizes to adjust with jawbone geometries. Recently, manufacturers have considered individual models for different bone types. Increasing implant surface area causes

better stress distribution and encourages osseointegration. Factors involved in success or failure of dental implants are implant mechanical strength, material biocompatibility, osseointegration degree of bone-implant interface, soft tissue adaptation to implant body, and implant capability of load transfer within tolerance levels [6]. However, marketing considerations have been influential in the design development of current implants rather than scientific studies.

To predict the failure area in the finite element method (FEM), principal and Von-Mises stress criterion would be used. When the maximum normal stress exceeds the ultimate stress, bone failure occurs [7]. This definition can be used as a method to predict and identify the failure regions due to either compression or tension [8].

In an FEA study, the maximum normal stress distribution of surrounding bone was calculated and regions, where the maximum principal stresses (tensile) were greater than 100 MPa and the minimum principal stress (compressive), was greater than 170MPa, recognized as overloaded area and local failure [9]. Boccaccio et al reported the accuracy of FEM for both orthotropic and isotropic models could be affected by up to 200% by definition of boundary conditions [10]. To stimulate bone remodeling stress, strain, strain energy density, and fatigue microdamage have been used in dentistry. The continuum strain energy density level per mass density ($U/\rho$) characterizes the stored energy at the bone tissue level [11, 12]

In recent years, many investigations on conventional implants have analyzed design factors using, with a concentration on major parameters such as diameter, pitch, and implant outlines in the distribution of stress in the bone-implant interface. There is still a need to understand the relationship and interaction of design factors individually with stress distribution to optimize implant structure. This study aimed to introduce, develop, and analyze a new dental implant and investigated the effect of design parameters on stress distribution. Therefore, finite element modeling was developed to facilitate the study with a comparison of design parameters. Boundary and loading conditions were implemented to simulate the natural situation of occlusal forces. The FEA simulated the natural masticatory situation of the Human jawbone.

## 2. Materials and methods

### 2.1. Implant modeling

The design structure of Zimmer and MegaFix dental implant systems inspired the primary idea of the new implant. Zimmer implant has a combination of spherical deeps on the surface and rectangular holes at the bottom. MegaFix implant consists of two different thread configurations for better stability. Therefore, the primary design was inspired by wall roll-plug construction. Once wall plug is inserted in the socket, fin edges stuck to the wall and provide residual stress and minimum mobility. Hence, the primary design aimed to produce residual stress generated from initial tightening torque. By considering conventional dental implants in the market and also inspiring from wall plug structures, a final model was designed using SolidWorks software (Figure 1).

The introduced design consisted of a cylindrical screw thread shape at the top and 4 rounded step shapes similar to wall plugs at the tail. The diameter of steps decreased from top to bottom, simulating tapered-stepped implant. Four holes were considered inside the cylinder to allow easier travel of blood and bony tissues to improve the healing process. Besides, these holes could increase the bone-implant contact surface and bring more stability. The fins were considered for the implant-tail part. Seven threads could cover this area, so the number of sharp edges is reduced. General V-shape thread was selected for the thread shape, as it was the most common configuration in the implants industry. The implant fins were triangular-paddle shape to provide asymmetric configuration on top and downside of lockers. The assumption was compressive vertical load as the major occlusal force would be received by the oblique side of fins and distributed over a bigger area, so more favorable stress-distribution would exist over the implant surface. This structure can increase the anchorage characteristic of the implant and provide more even stress distribution and a higher amount of micro-motions.

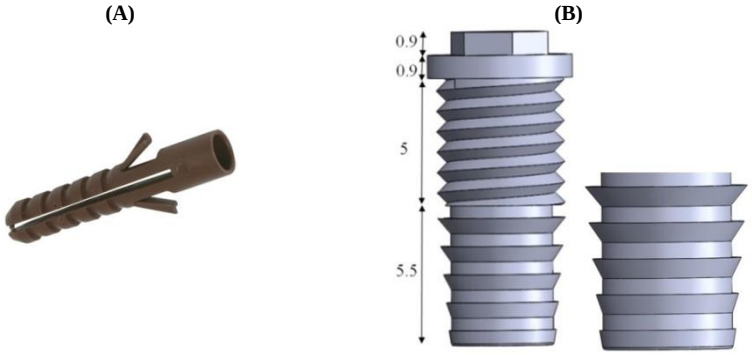


**Fig. 1:** (A) Plastic Wall Roll-Plug (B) Designed (V-5) Dental Implant Thread and Lockers Model.

The implant body had a diameter of 5 mm in the apex and 4 mm in the tail and 10.5 mm length. Implant head had a cylindrical-screw shape with a V-shape thread configuration. The thread shape was designed based on conventional V-shape threads with a maximum peak angle of 52.9º. The tail section consisted of five fin edges, which could be replaced by 7 to 8 threads with the same pitch configuration geometries. The first fin located in the middle of the implant body had the biggest diameter of 5 mm, the other fins diameters from top to tail were 4.8, 4.6, 4.4, and 4.2 mm, respectively. Since the diameter of the implant in the tail section was 4 mm, fins came out of the implant body and produce fin edges with depth of 0.5, 0.4, 0.3, 0.2, and 0.1 mm. The same thickness and internal distance of 0.6 mm and 0.5 mm were applied for all the fins (Table 1). To maximize the thread influence, the angle was determined to be $52.9^{O}$, which is the maximum possible angle. Table 2 presents specification of designed implant.

**Table 1:** Designed (V-5) Implant System Dimensions

| Up to down | Fin 1 | Fin 2 | Fin 3 | Fin 4 | Fin 5 |
|---|---|---|---|---|---|
| Upper Diameter (mm) | 5 | 4.8 | 4.6 | 4.4 | 4.2 |
| Edge Size (mm) | 0.5 | 0.4 | 0.3 | 0.2 | 0.1 |
| Oblique Side (mm) | 0.74 | 0.72 | 0.67 | 0.63 | 0.61 |
| Head Angle (degree) | 47.8 | 51.9 | 55.2 | 57.0 | 57.3 |

**Table 2:** Specification Of Designed (V-5) Implant

| Abutment Connection | Apical Features | Apical Shape | Body Feature | Body Shape | Cervical Feature | Cervical Shape |
|---|---|---|---|---|---|---|
| Eternal | Grooved | Flat apex | Threaded | Tapered | Polished Surface | Wider than body |

Branemark MK IV was modeled to validate introduced design (Figure 2). This implant is one of the most common and reliable products of Nobel Biocare Company. Specifications of Branemark MK IV were presented in Table 3. Branemark MK IV with 5 mm diameter, 10.5 mm length, 0.8 mm pitch size, and 0.4 mm thread depth was selected for modeling. In the tail section of Branemark MK IV, sharp edges of threads at the end of the implant were replaced by more curved edges to improve osseointegration in trabecular bone. The implant body had straight walls in the apex and tapered shape at the tail.

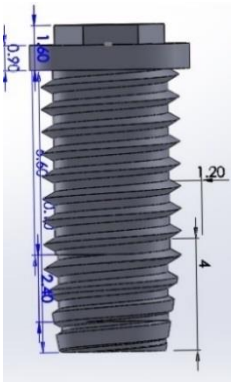


**Fig. 2:** Branemark MK IV.

**Table 3:** Branemark MK IV Specifications

| Branemark | Abutment Connection | Apical Feature | Body Feature | Cervical Feature | Surface Material |
|---|---|---|---|---|---|
| MK IV | External | Grooved | Threaded | Polished Surface | TPO |
| Abutment type | Apical Shape | Body Shape | Thread Shape | Cervical Shape | Implant Material |
| External Hex | Flat Apex | Tapered | V-shape | Wider than Body | Titanium Grade 4 |

The implant thread is V-shape with a tapered curve at the tail. Though, the shape of the threads is different from the V-5 implant model, in case of apex angle and the flat area between threads. Table 4 presents the geometrical data of two implant models. The final implant models were exported as STL format to be readable by 3-Matic software.

**Table 4:** Geometrical Properties of the Implant Models

| | Branemark | V-5 |
|---|---|---|
| Area ($mm^2$) | 286 | 277.98 |
| Volume ($mm^3$) | 699.45 | 690.27 |
| Weight (g) | 3.2 | 3.1 |

## 2.2. Jawbone modeling and assembly

A three dimensional (3D) human mandible model was constructed using Mimics software. The model was constructed by the use of 418 cross-sectional slices of computerized tomography (CT) scan images with field of view (FOV) of 150.00 mm and slice distance of 0.359 mm. The CT scan images belonged to a 34 years old male patient with 512 x 512 pixels resolution (Figure 4). To study the bone behavior with the highest possible accuracy, the inner and outer sides of bone were simulated based on the density distribution of cortical and cancellous bone. The second molar place in the left-wing of the jaw model was filled to prepare the model for implant insertion. It was assumed that the tooth cavity is recovered and filled up by bony tissues so; the inserted implant would be placed in a pre-filled bone area.

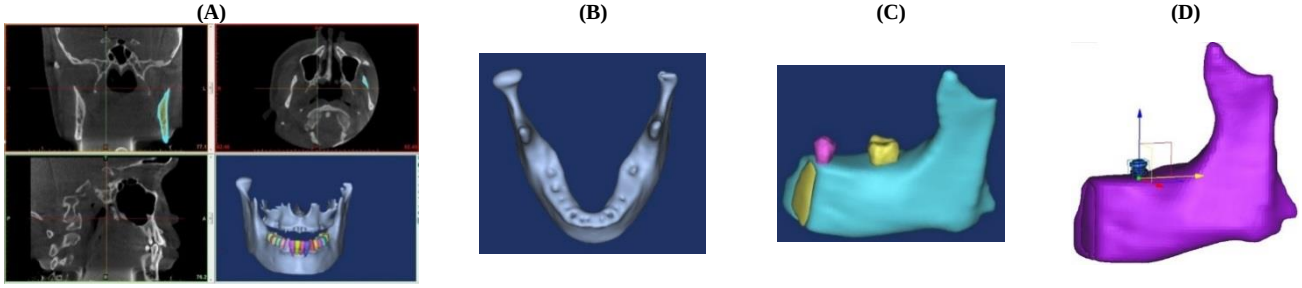


**Fig. 4:** (A) Axial, Sagittal and Coronal Views of the Jawbone (B) Filled Up the Position of the Left Second Molar in Full Human Jawbone Model in Mimics (C) Position of the Second Molar in Quarter Mandible Model (D) Branemark Implant Inserted Vertically Into Quarter Jawbone Model in 3-Matic

Though this model represents the full human jawbone model, the influence of biomechanical interactions in the bone-implant interface is limited to the implant surrounding area. Accordingly, to minimize the model analyses, the left quarter of the jaw was separated which includes the desired amount of area for FEA on the left molar tooth position. Once the left wing was separated, a 2 mm cortical bone layer was separated from cancellous bone representing bone type II. The final implant and bone models were imported to 3-Matic software for assembling. The implant models were inserted vertically into the bone model.

## 2.3. Analysis

Once two implants were inserted into the quarter jawbone model, the surface was meshed and smoothed to prepare for Abaqus software. Re-meshing was the final operation before exporting to Abaqus to reduce the triangles and amount of details while improving the quality of the model. This procedure in re-meshing repeated until the mesh quality displayer demonstrated the lower geometrical error of 0.3. The current modeling reached a geometrical error of 0.1, which is acceptable in Abaqus software. Abaqus software measured the stress and strain in the bone-implant interface. The principal stresses demonstrate the potentiate area of local fractures, the Von-Misses stresses show the stress growing areas, and finally, the strain analyses display the micro-motion of the bone considering the allowable displacement. The solution method was selected as dynamic explicit to let the force to be exerted in increments and lead to more accurate results. Furthermore, this method provides more convergence which increases the chance of obtaining results. Dynamic Explicit mathematical algorithm is described in the following:

Newton's Second Law: $F = ma$ (1)

Displacement (u) at $t = t_n$ $u_n^h = u_{n-1}^h + \theta_t u_{\frac{n-1}{2}}^h \Delta T$ (2)

Force calculation (F): $\varepsilon_n^h = \varepsilon(u_n)$,

$\sigma_n^h = E\varepsilon_n^h$, (3)

$F^h = F(u, \sigma^h, t)$ (4)

Acceleration calculation (A): $A_n^h = \theta_{t^2} u_n^h = M^{-1} F_n^h$ (5)

Velocity calculation (V): $V_{\frac{n+1}{2}}^h = \theta_t u_{\frac{n+1}{2}}^h = \theta_t u_{\frac{n-1}{2}}^h + A_n^h \Delta t$ (6)

E = Young modulus, Δt = time increment, ε = strain, σ = stress

Once the models were imported from 3-Matic to Abaqus, the models were assembled according to their definition in 3-Matic. As the models had surface meshing, Abaqus could convert and recognize the 3-D reconstruction of volumetric meshed models accurately as defined in 3-Matic. Besides, all the incomplete shapes and sharp counters were repaired in 3-Matic. Therefore, the solid models reconstructed in Abaqus without error. All the materials in this study were assumed isotropic, linear and homogenous, and elastic (Table 5). The trabecular bone was assumed to have a solid structure shielded by evenly 2 mm of cortical bone. Similar assumptions were applied for cortical bone and Titanium alloy (Ti–6Al–4V) with higher accuracy.

**Table 5:** Material Properties for Different Components in Abaqus

| Material/Properties | Density ($\frac{gr}{cm^3}$) | Young Modulus (MPa) | Poisson ratio |
|---|---|---|---|
| Titanium | 4.5 | 110000 | 0.3 |
| Cortical | 2 | 13700 | 0.3 |
| Cancellous | 1 | 1370 | 0.3 |

To simplify the modeling, only normal and tangential behaviors were considered and thermal properties were ignored. Hard contact behavior was defined under pressure for normal interaction between different parts. The friction coefficient was assumed at 0.35 [13]. So, only pressure, tangential and shear forces are transferred to the interface, and not tangential loads [14]. Surface-to-surface contact features of Abaqus with a friction coefficient of 0.35 defined the physical interactions at cortical bone-implant and cancellous bone-implant interfaces. It was assumed that the bone-implant and cancellous-cortical interfaces are bonded perfectly that indicates 100% osseointegration in the mutual interface. The boundary fixations included all degrees of freedom of the nodes located at the most external distal and mesial locations of the model (Figure 6). The boundary conditions were defined for all the nodes of the 3D model to restrain all degrees of motion.


**Fig. 6:** (A) Boundary Fixations of the Model in Abaqus (B) Use of 0.01mm Displacement as A Function of Load in Abaqus.

Two sets of static loads in vertical and tangential planes were simulated to analyze the influence of each force on generated stress in the bone-implant interface. The vertical forces of 50 (Cyclic) and 150 (Static), plus a tangential static force with components of (-50, 75, 0) N were applied on the implant model separately. Therefore, 90 N in a horizontal plane and 150 N in the vertical plane would lead to an Oblique load of 175 N. To increase the accuracy of the study, two equal displacements of 0.01 mm as Push-in and Pull-out loads were applied on the implant models individually. The displacement definition is higher than the normal movement of implants in one step; thus, they resemble extreme Push-in and Pull-out loading conditions (Figure 6 (b)).

# 3. Results

As different loading conditions were applied in the modeling, a wide range of factors was analyzed including the contact area between implant and surrounding bone, Von-Mises stress distribution over the bone-implant interface, principal stress magnitudes in the bone-implant interface, Von-Mises stress distribution over the implant body surface, induced micro-motion in cancellous and cortical bone. Stress and strain distribution under different loading conditions can be used as functional criteria to compare and analyze implant models. Micro-motions must be kept within a threshold of 50 to 150 µm as tolerated strain within the first year of insertion. The loading conditions were static compressive 150 N, cyclic compressive 50 N, static horizontal 50 and 75 N, Pullout, and Push in displacement of 0.01 mm. Final results were categorized in case of Von-Mises stress, Principal stress, and micro-motion.

## 3.1. Static compressive loading

Distribution of Von-Mises stress over the cortical bone in Branemark is uniform with an average magnitude of 60 MPa (Figure 7 (a)). Stress concentration happened along the edge of the first thread with a peak value of 120 MPa. Principal stresses were well distributed over all the threads with average and maximum of 85 MPa and 117 MPa respectively. In cancellous, stress was well distributed with an average amount of 8 MPa in the middle of the implant body and low-stress concentration over thread edges up to 12 MPa. In the tail, stress magnitude tended to increase in the lower threads. The highest amount of Von-Mises stress was 14 MPa and at the bottom of the implant. Similar to Cortical bone, principle stresses were more evenly distributed with an average magnitude of 7 MPa. Interestingly, the highest stress concentrations occurred around sharp edges in the middle of the implant and notches at the tail. Analysis of Von-Mises stress distribution over implant demonstrated that stress across the implant body is well distributed, with the highest stress concentration of 31.6 MPa at the first thread, 39.5 MPa in the middle of the body, and 31.6 MPa in the tail. Branemark implant in the cortical and cancellous bone under a static load of 150 N showed a micro-motion of 4.5 µm.

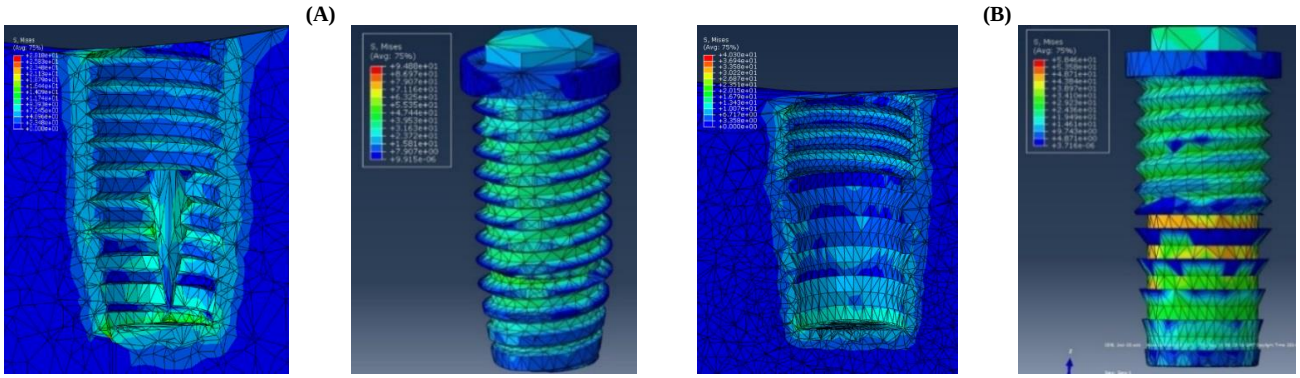


**Fig. 7:** Von-Mises Distribution of 150 N Static Force (A) in Cancellous Bone and Branemark Implant (B) in Cancellous Bone and V-5 Implant.

An average Von-Mises stress of 53 MPa was distributed over V shape threads in cortical bone (Figure 7 (b)). A high concentration of stress occurred in the first thread with a magnitude of 80 MPa. Principal stresses with an average of 54 MPa covered the threads area and first thread at implant neck had local stress concentration of 95 MPa over sharp edges. In Cancellous bone, V-5 demonstrated a stress magnitude of 13 MPa in the middle threads and maximum stress of 16 MPa over thread edges. In the tail Von-Mises, stresses were slightly higher with a magnitude of 16 MPa and a maximum of 20 MPa at the bottom. Principal stresses were well distributed over the implant body with the amount of 14 MPa and a higher amount of 20 MPa at the tail. Distribution of Von-Mises stress within the V-5 model showed stress concentration over thread area reaches 29.2 MPa and high-stress accumulation occurred in the middle of the body (48.7 MPa), and low stress at the tail. V-5 under this loading condition had a micro-motion of 5.2 µm in cortical and cancellous bone.

## 3.2. Cyclic compressive loading

Since human mastication activity is a repetitive loading and unloading process, one of the loading conditions was a cyclic compressive vertical load of 50 N on the implant body. The implant models were simulated under 2.5 cycles of compressive load, so at the end of the loading, the model was under pressure. The number of cycles was limited to 2.5 cycles to avoid massive processing time by Abaqus that usually yield to failure in termination of analyses. This section presents the stress distribution of bone-implant interface under a compressive cyclic load of 50 N. The amount of force was selected to represent the cyclic chewing habit of the human jawbone that is usually smaller in magnitude than biting forces.

Von-Mises stress over cortical bone was well distributed with some local stresses over thread edges (Figure 8). The average stress over cortical bone was 13.8 MPa with stress concentration over the first thread with a magnitude of 27.6 MPa. Principal stress was more evenly distributed over the thread area with the amount of 16.6 MPa and over the first thread with an amount of 38.7 MPa. Cancellous bone had average Von-Mises stress of 2.3 MPa in the middle of the implant body and 3.9 MPa over the tail and maximum of 4.9 MPa in the bottom. Principal stresses covered a range of 3.4 to 4.5 MPa over the bone interface. Von-Mises stress within the implant body showed a good distribution of stress with 10 MPa in the first thread, 13.1 MPa in the middle, and 5.2 MPa at the tail. Branemark implant had a strain micro-motion of 1.6 µm under 50 N cyclic loads in cortical and cancellous bone.

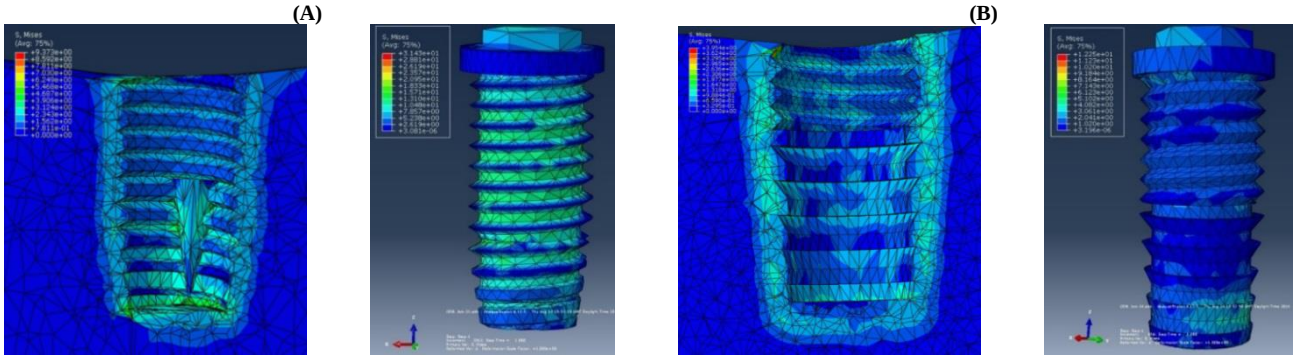


**Fig. 8:** Von-Mises Stress of 50 N Cyclic Force (A) in Cancellous Bone and Branemark Implant (B) in Cancellous Bone and for V-5 Implant.

V-5 implant model, in cortical bone, showed a very low Von-Mises stress of 4.1 MPa and stress concentration over first thread around 8.2 MPa (Figure 8 (b)). Principal stress had a similar pattern with an average value of 2 MPa and local stresses up to 8.5 MPa over the first and last threads. In cancellous bone, low Von-Mises stress of 0 to 1.3 MPa over implant body existed with the highest amount of 1.6 MPa in the tail. Principal stresses were almost zero in the majority of the contact area with some local stress concentrations less than 2 MPa. V-5 demonstrated a very low-stress magnitude over the implant body with 4.1 MPa in the first thread, 3.1 MPa in the middle, and a peak value of 6.1 MPa in the tail. V-5 implant produced a strain micro-motion of 2.6 µm in cortical and cancellous bone.

### 3.3. Static horizontal loading

For Branemark implant (Figure 9 (a)), in cortical bone, Von-Mises stress was about 22.6 MPa in the majority of the body with peak values of 45.2 MPa over sharp edges. In the first thread, Von-Mises stress concentration increased to 90.4 MPa. Principal stresses were not well distributed as previous cases, half of the implant was covered with 25.3 MPa and a half had 44.3 MPa. In the compressed areas of cortical bone, maximum stress concentration reached 63.2 MPa mostly around the first thread. In cancellous bone, most of the body had Von-Mises stress of 6.3 to 7.8 MPa and increased to a maximum of 11 MPa at the bottom of the implant. Principal stresses in the cancellous bone had a magnitude of 3 MPa to 5.2 MPa. Von-Mises stress was well distributed within the body, though; in the first and third thread, it reached a maximum of 28 MPa. In the middle, stress was around 15.5 MPa and reduces to 9.3 MPa in the tail. This implant has a micro-motion of 2.7 µm under horizontal loading.

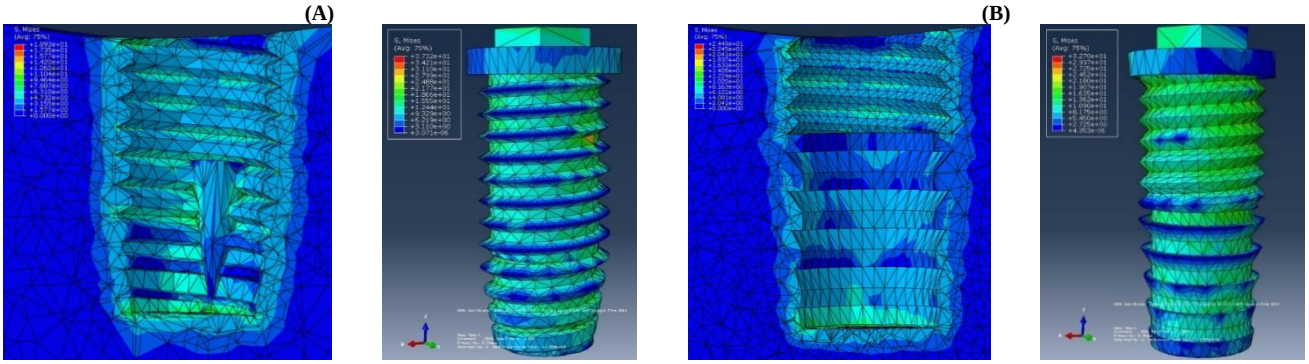


**Fig. 9:** Von-Mises Stress of Horizontal Force (A) in Cancellous Bone and Branemark Implant (B) in Cancellous Bone and V-5implant.

For V-5 implant (Figure 9 (b)), in cortical bone, Von-Mises stress over threads was around 22.5 to 45 MPa with a peak value of 56.3 MPa in the first thread and some local stress concentration up to 90.2 MPa. Principal stresses were 32.7 MPa over threads and 56.6 MPa in the first thread. In cancellous bone, the V-5 model showed 8 to 10 MPa Von-Mises stresses in the thread area and lower stress between 4 to 6 MPa over the fins. At the bottom of the implant, it reached the highest point of 12.2 MPa. In the case of principal stresses, this implant produced 6.4 MPa with the highest value of 7.7 MPa at the bottom of the implant. Von-Mises stress in implant body had high concentration over thread area with a magnitude of 21.8 MPa, in the middle reached 16.3 MPa, and finally over tail covered a range of stress between zero to 2.7 MPa.V-5 implant under Horizontal loading condition had strain micro-motion of 3.2 µm.

### 3.4. Pull-out displacement

One of the common methods in stress analyses is applying displacement and measuring of generated stress within the sample. The fourth loading condition set up as a vertical pull out the displacement of 0.1 mm. This displacement is higher than normal implant motion; therefore, it is considered as extreme loading condition like biting a stiff material and can demonstrate pullout strength of implant under a high amount of force.

Displacement of 0.01 mm of Branemark implant caused Von-Mises stress distribution in cortical bone with average values of 57.6 MPa and 115.3 MPa in the first thread (Figure 10 (a)). Principal stresses showed an even distribution over implant body with a magnitude of 37 MPa, though in the adjacent bone the peak local value reached 123.1 MPa. In cancellous bone, in the thread area, the average Von-Mises stress was less than 7 MPa and in the tail, it reached 13.5 with a peak value of 20 MPa in the bottom. Principal stresses in the middle of the body were about 4.5 MPa and reached 8.9 MPa in the tail. Von-Mises stress within the implant body showed 158.6 MPa in the first thread, 126.9 MPa in the middle, and 95.1 MPa at the tail.

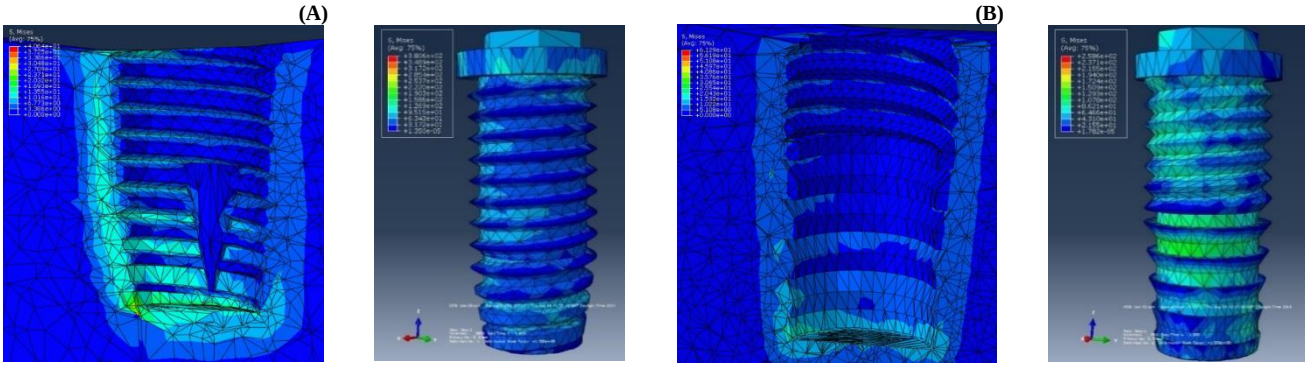


**Fig. 10:** Von-Mises Stress for Pullout Displacement of 0.01 Mm (A) in Cancellous Bone and Branemark (B) in Cancellous Bone and V-5implant.

In the V-5 Model (Figure 10 (b)), Von-Mises stress over threads in cortical bone was about 31 MPa and reached 41.4 MPa in the first thread. Principal stress in the first thread was 40.3 MPa; however, the average value over the majority of threads was 16.3 MPa. In cancellous bone, Von-Mises stress over threads was 5.1 MPa and reached 10.2 MPa in the sharp edges of threads. In the tail, this implant showed slightly higher stress around 20.4 MPa at the bottom. In the case of principal stresses, the majority of V-5 implant was covered with 8.5 MPa over threads with a peak value of 20.6 MPa in the bottom. Von-Mises stress concentration occurred in the middle of the implant above the first two fins with a magnitude of 129.3 MPa, threads had the stress of 86.2 MPa and at the tail, the low-stress concentration of 43.1 MPa happens.

### 3.5. Push-in displacement

Similar to Pull-out, a Push-in displacement of 0.01 mm vertical downwards was applied on each implant's body to observe the generated stress in the surrounding bone (Figure 11). For Branemark implant, in cortical bone, the generated stress under 0.01 mm pushing would yield to 49.6 MPa Von-Mises stresses over thread area with a peak magnitude of 99.3 MPa in the first thread. Principal stresses in cortical bone were 43 MPa over threads with a peak value of 115 MPa in the first thread. However, in some minor locations of the surrounding bone, local stress went up to 186.9 MPa. In cancellous bone, the middle of the implant had Von-Mises stress of 10.1 MPa and in the tail, it reached 13.5 MPa, and the highest stress concentration in the bottom occurred at magnitude of 20.2 MPa. Principal stresses, in cancellous bone, over threads were 6.3 MPa and in the tail reach to 10 MPa with a peak magnitude of 13.4 MPa at the bottom. Von-Mises stress distribution over the implant showed the highest stress concentration occurs in the first thread with a magnitude of 127.2 MPa. Other threads had well-distributed stress of 95.4 MPa.

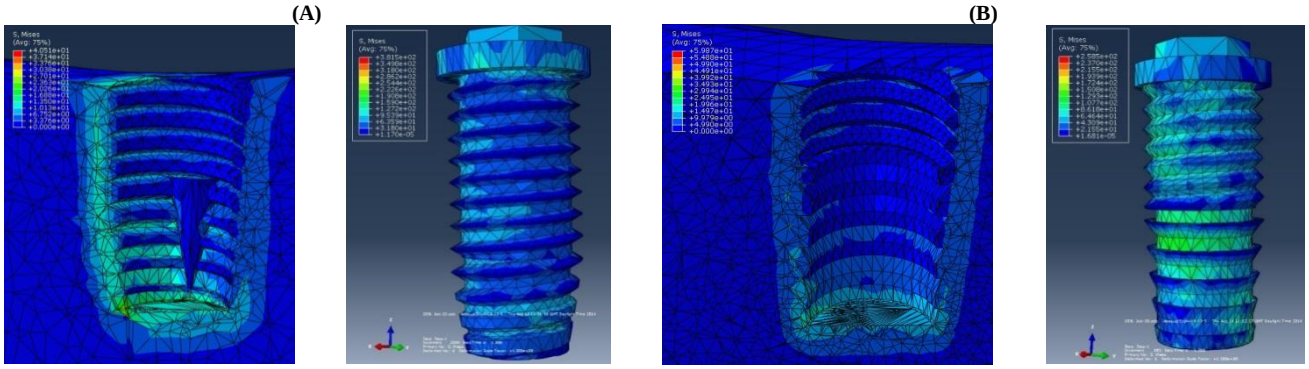


**Fig. 11:** Von-Mises Stress for Pushin Displacement of 0.01 Mm (A) in Cancellous Bone and Branemark Implant (B) in Cancellous Bone and V-5implant.

For V-5 implant, Von-Mises stress in the cortical bone had an average value of 42.7 MPa with a stress concentration of 74.7 MPa in the first thread. Principal stresses in the first thread came to a maximum of 64 MPa and had an average value of 27.1 MPa over other threads. The upper side of the V-5 implant in the cancellous bone had Von-Mises stress of 5 MPa with local stress concentration over sharp edges with a magnitude of 10 MPa. Over the tail, Von-Mises stresses reached 15 MPa with the highest magnitude of 25 MPa at the bottom. Principal stresses over the implant body had an average value of 10 MPa, however, in the surrounding bone; it reached to 16.6 MPa. Von-Mises stress pattern within the implant body represented a low rate of stress contribution from 21.5 to 107.7 MPa over threads, which showed uneven stress distribution. The first and second fins had the highest stress concentration of 129.3 to 150.8 MPa. At the tail, the magnitude of stress reduced to 43 to 64.6 MPa.

Table 6 shows stress under loading conditions for the Branemark implant. The first and second lines in Von-Mises stress row come from bone and implant stress analyses respectively. Since principal stress of implant is not considered; the second line of this row is left blank. Induced strain row for Pull-out and Push-in displacements are left empty because the amount of micro-motions is equal to 0.01 mm, which is not considered as induced strain. In overall, Branemark implant system showed a well distribution of stress under different loading conditions and also high stability inside the bone. Similarly, Table 7 displays stress magnitudes of V-5 implant under different loading settings.

**Table 6:** Stress and Strain Magnitudes of Branemark

| Branemark | (0, 0, -150) N | (0, 0, 50) N | (-50, 75, 0) N | +0.01 mm | -0.01 mm |
|---|---|---|---|---|---|
| Von-Mises Stress Cortical (MPa) | 60, 120<br>31 | 13.8, 27.6<br>10 | 22.6, 45.2<br>90 | 57.6, 115.3<br>158.6 | 49.6, 99.3<br>127.1 |
| Principal Stress Cortical (MPa) | 117, 85<br>----- | 16.6, 38.7<br>----- | 25.3, 44.3, 63.2<br>----- | 37, 123.1<br>----- | 43, 115, 186.9<br>----- |
| Von-Mises Stress Cancellous (MPa) | 8, 12, 14<br>39.5, 31.6 | 2.3, 3.9, 4.9<br>13.1, 5.2 | 6.3, 7.8, 11<br>15.5, 9.3 | 7, 13.5, 20<br>126.9, 95.1 | 10.1, 13.5, 20.2<br>95.4 |
| Principal Stress Cancellous (MPa) | 7<br>----- | 3.4, 4.5<br>----- | -3, 5.2<br>----- | 6.3, 10, 13.4<br>----- | 10, 16.6<br>----- |
| Induced Strain (μm) | 4.5 | 1.6 | 2.7 | ----- | ----- |

**Table 7:** Stress and Strain Magnitudes of V-5 Implant

| V-5 | (0, 0, -150) N | (0, 0, 50) N | (-50, 75, 0) N | +0.01 mm | -0.01 mm |
|---|---|---|---|---|---|
| Von-Mises Stress Cortical (MPa) | 53, 80<br>29.2 | 4.1, 8.2<br>4.1 | 22.5, 45, 56, 90<br>21.8 | 31, 41.4<br>86.2 | 42.7, 74.7<br>107.7 |
| Principal Stress Cortical (MPa) | 54, 95<br>----- | 2, 8.5<br>----- | 32.7, 56.6<br>----- | 40.3, 16.3<br>----- | 64, 27.1<br>----- |
| Von-Mises Stress Cancellous (MPa) | 13, 16, 20<br>48.7, 14.6 | 1.3, 1.6<br>3.1, 6.1 | 8, 10, 12.2<br>16.3, 2.7 | 5.1, 10.2, 20.4<br>129.3, 43.1 | 5, 10, 15, 25<br>150.8, 64.6 |
| Principal Stress Cancellous (MPa) | 14, 20<br>----- | 0, 2<br>----- | 6.4, 7.7<br>----- | 8.5, 20.6<br>----- | 10, 16.6<br>----- |
| Induced Strain (μm) | 5.2 | 2.6 | 3.2 | ----- | ----- |

## 4. Discussion

This study investigated the influence of design parameters of dental implants in stress distribution to find optimized design criteria and introduce a new implant. Finite element modeling in this study provided a wide range of loading settings to assist in the evaluation of implant design parameters in different conditions. V-shape threads with maximum apex angle had low strength in the cortical bone which generates a high rate of strains. Low Von-Mises stress discouraged remodeling and strengthening of bone. It seems the absence of a gap between threads caused less bone integration and a higher range of movement. In cancellous bone, V-shape threads had the lowest performance. Low amount of Von-Mises stress, accumulation of local principal stress and high rate of motion under different conditions could lead to early failure. V-5 fin had no extraordinary performance in cancellous bone. Small surface areas of fins did not integrate with the surrounding bone and high-stress concentration occurred at the tail. These fins are recommended as threads replacement.

In this study, various loading settings were considered; 150 N vertical static, 50 N vertical cyclic, 50 N and 75 N combined horizontal loading in buccal-lingual plane, 0.1 mm Pull-out displacement, and 0.1 mm Push-in displacement. FEA performed in two groups of implants including V-5 and Branemark. The FEA results were analyzed based on stress distribution within the Cortical, Cancellous, and implant interface. The stress distribution of models was assessed based on three major elements; Von-Mises stress, principal stress, and induced strain

Dental implants have been implemented widely over last few decades with high satisfactory success rate. However, high rate of failure is reported for low bone densities. Though, implant design has shown to have great influence on generation and distribution of stress over bone implant interface, implant development and design analyses have been restricted to conventional implants in the market. Dental implants are made of ductile materials with high yield stress much bigger than bone ultimate stress, consequently, implant fracture does not occur within a defined range of forces. Therefore, the implant interface was analyzed based on only Von-Mises stress distribution. These factors were measured and evaluated in five major areas; first thread in cortical bone, thread area in cortical bone, first thread in the cortical-cancellous interface, thread area in cancellous bone, fins area in cancellous bone, and implant bottom in cancellous bone.

Branemark MK IV as an approved implant available in the market was chosen as the control group and results were evaluated based on the performance of this implant. Overall, the Branemark implant system showed good distribution of stress under different loading conditions and also high stability inside the bone.

V-5 implant had a V-shape thread similar to Branemark but with a maximum apex angle of 52.9º that causes the absence of a gap between threads, which exists in Branemark. Under static load, the generated stress was not well distributed comparing to Branemark results. The average Von-Mises stress was quite low and the first thread was under a high amount of stress concentration. A similar pattern was seen in principal stress distribution. Though Branemark showed some stress concentration over the first thread, stress was well distributed and no critical area existed. However, V-5 generated uneven principal stress, which could cause bone fracture over the first and last thread in cortical bone.

In a cyclic load, V-5 generated a minimum amount of Von-Mises stress in the test group. The pattern of principal stresses confirms low resistance under vertical load. Under horizontal loading, V-5 demonstrated better functionality. Though Von-Mises stress distribution had slightly lower magnitude, the distribution of stress was more even comparing with vertical loading. In the case of principal stress, V-5 showed high-stress concentration over the first thread and less uniform distribution comparing to Branemark.

In overall, Von-Mises stress under vertical and horizontal loading did not display a well-distributed pattern. This implant represented low resistance under vertical load and high concentration of stress in the first thread and in the bone layers interface. 0.01 mm displacement is representative of extreme loading conditions. Therefore, a higher amount of stress means higher stability and strength of the implant. Comparison of generated stress in both Push-in and Pull-out demonstrated very low resistance of V-5 thread under dislocation. Though principal stress in V-5 had much lower magnitude in both cases, it was not well distributed and high local stress concentration existed in the adjacent bone.

In cancellous bone, the V-5 implant demonstrated a higher rate of stress under static 150 N force. This can be caused by a lower rate of stress in cortical bone. Although threads showed good distribution of stress, the generated stress was almost two times bigger than the Branemark model. Von-Mises stress distribution over 7 threads of Branemark exhibited lower stress over fins than threads compared to 5 fins of V-5 model. On the other hand, at the bottoms, V-5 had slightly higher stress concentration. Principal stress patterns also showed higher stress in cancellous bone for V-5 compared to Branemark. Possibility of bone fracture in the cortical-cancellous interface and at the bottom was higher than other areas in the V-5 implant.

Under cyclic load, V-5 had low Von-Mises stress with local stress concentration in the cortical-cancellous bone interface. Based on the results, stress over fins was almost equal to zero. Threads had higher stress, though much lower than Branemark threads. Principal stress-

es had low magnitude, though there was a high concentration in bone layers interface. Under horizontal loading, the V-5 implant showed better performance. The magnitude of Von-Mises stress over threads was close to Branemark, though fins in the middle of the implant had less stress concentration. Consequently, the implant bottom had more stress under loading and displayed high-stress values.
Von-Mises results for Pull-out and Push-in conditions in cancellous bone showed that average stress is lower than Branemark, however, there was a high local concentration in V-5 implant. V-5 implant in the fin area had less integration with the cancellous bone that yield to low-stress concentration and accumulation of stress at the bottom. Principal stresses had slightly bigger values with higher accumulation over the last two fins.V-5 implant showed less stress in the cortical bone that causes high-stress concentration in cancellous bone. This performance under vertical loading and displacement was brighter. This is in agreement with a high rate of induced strain, which is more than two times of Branemark generated strains. However, under horizontal loads, this implant showed acceptable functionality and induced a lower rate of strains. Based on results, V-shape threads in the cortical bone had a higher rate of movement that leads to less stress distribution in cortical bone and more stress generation in cancellous. Besides, V-5 fins did not integrate with surrounding bones and assisted less stress accommodation.
Several limitations were observed in this study. Using oblique loading and bending moment in FEA may present more reliable results. Furthermore, using different bone types may support the contribution of the optimized implant stronger. A wide range of recommendations can be stated for future extensions of the introduced approach in this study. Surface roughness can be analyzed to increase the contact area in the interface. The effect of the design parameters of implants can be investigated on fatigue endurance. By using glue and composite materials, the long life expectancy of dental implants can be analyzed.

## 5. Conclusion

The FEA results can determine the geometrical influence of implant design under different loadings. FEA as a repetitive analytical method was implemented to display stress distribution patter along with the bone-implant interface. Based on the results, V-shape threads with maximum apex angle caused a high rate of micro-motion and a high possibility of bone fracture. Low Von-Mises stress was associated with low bone growth stimulation. Besides, small fin threads did not integrate with cancellous bone and consequently lower stress accommodation. Based on FEA results, implant structure had less influence on stress distribution under horizontal loading.

## Acknowledgement

We acknowledge Global College of Engineering and Technology of Oman for supporting the study

## References

[1] Haas R, Mailath-Pokorny G, Dörtbudak O, Watzek G, Polak C & Fürhauser R (2002), "A long-term follow-up of 76 Brånemark single-tooth implants", *Clinical oral implants research*, Vol. 13, No. 1, pp.38-43. https://doi.org/10.1034/j.1600-0501.2002.130104.x.
[2] Christensen GJ (2002), "Implant prosthodontics: from single tooth to complex cases", *Journal of Oral Implantology*, Vol. 28, No. 5, pp. 244-248. https://doi.org/10.1563/1548-1336(2002)028<0244:IPFSTT>2.3.CO;2.
[3] Morgan M & James D (1995), "Force and moment distributions among osseointegrated dental implants", *Journal of Biomechanics*, Vol. 28, No. 9, pp.1103-1109. https://doi.org/10.1016/0021-9290(94)00139-U.
[4] Li W, Lin D, Rungsiyakull C, Zhou S, Swain M & Li Q (2011), "Finite element based bone remodeling and resonance frequency analysis for osseointegration assessment of dental implants", *Finite Elements in Analysis and Design*, Vol. 47, No. 8, pp.898-905. https://doi.org/10.1016/j.finel.2011.03.009.
[5] Çehreli M, Şahin S, & Akça K (2004), "Role of mechanical environment and implant design on bone tissue differentiation: current knowledge and future contexts", *Journal of dentistry*, Vol. 32, No. 2, pp.123-132. https://doi.org/10.1016/j.jdent.2003.09.003.
[6] Frost HM (1994), "Wolff's Law and bone's structural adaptations to mechanical usage: an overview for clinicians", *The Angle Orthodontist*, Vol. 64, No. 3, pp.175-188.
[7] Mendelson A "*Plasticity: theory and applications*". New York (1968)
[8] Bozkaya D, & MuftuS, Muftu A (2004), "Evaluation of load transfer characteristics of five different implants in compact bone at different load levels by finite elements analysis",*The Journal of prosthetic dentistry*, Vol. 92, No. 6, pp.523-530. https://doi.org/10.1016/j.prosdent.2004.07.024.
[9] Martin RB, Burr DB, & Sharkey NA "*Skeletal tissue mechanics*". Springer (1998) https://doi.org/10.1007/978-1-4757-2968-9.
[10] Boccaccio A, Lamberti L, Pappalettere C, CaranoA, & Cozzani M (2006), "Mechanical behavior of an osteotomized mandible with distraction orthodontic devices", *Journal of Biomechanics*, Vol. 39, No.15, pp.2907-2918. https://doi.org/10.1016/j.jbiomech.2005.09.016.
[11] Chou H, Jagodnik JJ & Müftü S (2008), "Predictions of bone remodeling around dental implant systems", *Journal of Biomechanics*, Vol. 41, No. 6, pp. 1365-1373. https://doi.org/10.1016/j.jbiomech.2008.01.032.
[12] Huiskes R, Weinans H, & Van Rietbergen B (1992), "The relationship between stress shielding and bone resorption around total hip stems and the effects of flexible materials", *Clinical orthopaedics and related research*, Vol. 274, pp. 124-134. https://doi.org/10.1097/00003086-199201000-00014.
[13] Kayabaşı O, Yüzbasıoğlu E, & Erzincanl F (2006), "Static, dynamic and fatigue behaviors of dental implant using finite element method", *Advances in Engineering Software;* Vol. 37, No. 10, pp.649-658. https://doi.org/10.1016/j.advengsoft.2006.02.004.
[14] Ding X, Liao S, Zhu X, Zhang X, & Zhang L (2009), "Effect of diameter and length on stress distribution of the alveolar crest around immediate loading implants", *Clinical implant dentistry and related research*, Vol. 11, No. 4, pp. 279-287. https://doi.org/10.1111/j.1708-8208.2008.00124.x.